

doi: 10.11933/j.issn.1007-9289.20230227003

10 m 长管道内壁类金刚石薄膜沉积及性能*

靳朋礼^{1,2} 田修波¹ 巩春志¹

(1. 哈尔滨工业大学材料科学与工程学院 哈尔滨 150000;
2. 东莞松山湖材料实验室 东莞 523000)

摘要: 工业生产过程中管道内壁经常受到输送物质的腐蚀和磨损, 对管道内壁进行涂层防护十分必要, 而目前鲜有在大长径比管道内壁镀膜的报道, 且缺乏对大长径比管道内壁膜层性能的研究。采用等离子体增强化学气相沉积(PECVD)技术在直径100 mm、长10 m管道内壁沉积类金刚石(DLC)薄膜, 并研究管道内工作气体的等离子体放电辉光光谱、膜层表面亮度、水静态接触角、硬度、摩擦因数和拉曼光谱等。结果表明: 管道内等离子体光谱显示管内等离子体中有Ar⁺和乙炔分解成的C₂、H和CH; 膜层表面的亮度L*最高达到37.4和色差ΔE*最大1.9, 膜层拉曼光谱结果表明靠近管道两端和中间位置膜层的I_D/I_G均匀, 膜层水静态接触角显示靠近管道两端的膜层接触角略小; 靠近管道两端膜层硬度相比中间位置的膜层硬度高, 并且磨损测试中膜层均未出现破损剥落, 膜层具有高的耐磨性。试验实现了在大长径比的管道内壁沉积耐磨损的DLC膜层, 为长管道内壁均匀镀膜提供了理论支持和技术指导。

关键词: 等离子体增强化学气相沉积(PECVD); 长管道; 内壁镀膜; 类金刚石

中图分类号: TG156; TB114

Deposition and Properties of DLC Film on the Inner Wall of a 10-m-Long Stainless-steel Tube

JIN Pengli^{1,2} TIAN Xiubo¹ GONG Chunzhi¹

(1. School of Materials Science and Engineering, Harbin Institute of Technology University,
Harbin 150000, China;
2. Songshan Lake Materials Laboratory, Dongguan 523000, China)

Abstract: During industrial production, the inner wall of a tube is often corroded and worn by the conveying material; therefore, it must be protected. Currently, research on the coating of the inner wall of a tube is limited, and research regarding the performance of the inner wall of a large-aspect-ratio tube is lacking. Thus, this study attempts to solve the problem of a diamond-like carbon(DLC) film on the inner wall of a long tube. Herein, the internal surface of a 304 stainless-steel tube, which is 10 m long and 100 mm in diameter, is coated with DLC using plasma-enhanced chemical vapor deposition(PECVD). The hollow cathode discharge of gas into the tube, brightness of the film, contact angle, surface hardness, friction factor, and Raman spectroscopy results are characterized using different tests. During the preparation of the inner coating, the plasma spectrum in the 300–800 band at position 3 of the pipe is analyzed using a spectrometer and optical focusing platform. After the film is prepared, its surface brightness is measured using a color difference meter to determine the L*, a*, and b* values of the film, where L* represents the brightness, a* represents red and green, and b* represents yellow and blue. Scanning electron microscopy(SEM) is used to observe the section morphology of the film. The surface roughness of the film is measured using atomic force microscopy(AFM). A friction and wear-testing machine is used to test the wear resistance of the film. A GCr 15 ball with a diameter of 3 mm is selected as the grinding pair, and the experimental parameters of load, rotational speed, and test time are set as 3 N, 200 r / min, and 120 min, respectively. A nanoindentation hardness

* 国家自然科学基金(12075071, U2241233)、黑龙江省头雁创新团队计划(HITY-20190013)和黑龙江省自然科学基金(LH2019A014)资助项目。

Fund: Supported by National Natural Science Foundation of China (12075071, U2241233), Heilongjiang Touyan Innovation Team Program (HITY-20190013), and Natural Science Foundation of Heilongjiang Province (LH2019A014).

20230227 收到初稿, 20230920 收到修改稿

instrument is used to measure the nanohardness of the film. A measuring meter for the static contact angle of water is used for measurement; the measurement requires 2 μl of each drop. Each sample is tested three times, and the average value is calculated as the final test result. The film is measured by a laser Raman spectrometer using a 532 nm laser source from 800 to 2 000 cm^{-1} , and a Gaussian curve is employed to fit the Raman spectrum. The results demonstrate that in the coating process of the inner wall, the first step is the entry of Ar gas into the pipe for glow discharge cleaning. Ionization and excitation occur during the process of Ar gas discharge, thereby producing Ar^+ and Ar^0 ; additionally, C₂, H, and CH decompose from acetylene. The SEM results of the cross-sections of the films at different positions reveal that the cross-section of the film is uniform and dense, with no cracks, pinholes, or other defects. Further, no cracks are observed in the binding transition between the film and matrix, thickness of the film at different positions, and thickness of the film near the ends of the pipeline, thus indicating that the plasma density in this region and the deposition rate of the film are high. The largest L^* and ΔE^* values of the film are 37.4 and 1.9, respectively. The AFM results demonstrate larger bulges on the film surface at positions 3 and 7, which result in high surface-roughness, and uniform distribution of the bulges at positions 3 and 9. The water contact angles of the films are smaller at both ends. The results of the wear tests indicate that the friction factor of the film decreases in the first 20 min from 0.225 to approximately 0.175. For a prolonged time, the friction factor remains stable at 0.17. The hardness of the film near the ends of the pipe is slightly higher. Further, no damage or film-peeling is noted in the pin-on-disk test, and the film is characterized as having a good wear resistance. The Raman spectra of the films at different positions reveal that in contrast to positions 1 and 9, the G peaks at positions 3 and 7 exhibit a shift toward the peak level, thus indicating a high stress in the film at both ends. Considering the distribution trend of I_D / I_G in the film, a low ratio of I_D / I_G is determined at both ends of the tube. The glow discharge and DLC deposition in the long tube with a large length ratio provides theoretical support and technical guidance for the uniform coating of the walls of long pipes.

Keywords: plasma enhanced chemical vapor deposition (PECVD); long tube; inner coating; diamond-like carbon

0 前言

管道作为工业传输系统的重要组成部分，广泛应用于石油化工、海洋工程、供水、污水处理等领域^[1]。但管道内输送的材料中含有酸、碱等物质，管道内壁发生腐蚀、磨损，带来了重大的经济损失^[2]。因此，研究人员采用了一系列涂层技术来解决这一问题，如喷涂^[3-4]、电镀^[5]、等离子体涂层技术^[6-8]等。在众多涂层技术中，采用等离子体涂层技术在管道内沉积类金刚石（Diamond-like carbon, DLC）薄膜取得了较好的效果，其原因是 DLC 薄膜具有高硬度、高化学惰性、低摩擦因数和磨损率，以及优良的耐腐蚀性^[9-11]。

目前，研究人员主要研究的是在长度为 20~200 cm 的管道内壁镀膜，且管道内壁膜层不均匀。对于大长径比（长度大于 2 m）的管道内壁均匀镀膜更是具有极大挑战。例如，PILLACA 等^[12]研究了在直径 10 cm、长 2 m 管道内，不同气体放电时等离子体的温度和进气与抽气形式对管内膜层厚度分布的影响。结果表明，进气与抽气方式直接影响膜层厚度的分布。WANG 等^[13]报道了在直径 56 mm、长 56 cm 的管道内进行沉积 DLC 薄膜，发现在管道一端进气另一端抽气时，膜层的厚度随进气方向逐渐减小。BABA 等^[14]在长 1 m、直径 35 和 20 mm

的管道内沉积 DLC 膜层，膜层的厚度随进气方向先增大后减小。以上研究显示出膜层在管内不均匀的问题，分析主要原因有：①管道较长，采用现有方式向管道内部导入气体，气体在管道内部分布不均匀，导致管道内气体放电时等离子体均匀性差，在管内制备的膜层厚度和性能差异较大，影响了管内壁膜层的使用效果。②管道过长过大时，由于地电阳极距离管道内部较远，管道内等离子体在阴极和阳极之间传输效率低，导致管道内部等离子体密度极低，甚至无法启辉，严重影响了管道内部镀膜，制约了长管道内部镀膜技术的发展与应用。

本文采用自主研制的长管道内壁镀膜设备与电源，利用等离子体增强化学气相沉积技术（Plasma enhanced chemical vapor deposition, PECVD）研究长 10 m、直径 100 mm 管道内壁 DLC 涂层沉积，探究影响 10 m 长管道内壁膜层沉积及其性能的因素。研究管道内工作气体辉光放电的光谱以及不同位置膜层的亮度、粗糙度、硬度、耐磨性、接触角和薄膜微观结构，为实际工业生产奠定理论基础。

1 试验准备

1.1 试验装置样品制备

试验装置为自行研发设计的长管道内壁镀膜设备，由机械泵、分子泵、真空腔室、管道组成。被

镀管道作为真空室的一部分。设备可对直径 50~300 mm、长 1~12 m 的管道内壁进行镀膜。镀膜电源为实验室自主研制的高压脉冲镀膜电源, 如图 1 所示, 电压 0.4~10 kV、频率 0~1.2 kHz。采用直径 100 mm、长 10 m 的 304 不锈钢管。硅片试样为 10 mm×10 mm 的样片, 用于检测 DLC 薄膜的厚度。不锈钢试样切割成 20 mm×20 mm 抛光后, 在室温下用无水酒精超声清洗 20 min, 再用去离子水冲洗干净, 吹风机吹干后, 在 10 m 管道内每间隔 1 m 放置一片, 编号 1~10。工作气体采用高纯度 Ar 气、高纯度乙炔、四甲基己硅烷(TMS), 纯度为 99.99%。镀膜工艺开始前真空室初始真空为 1.0 mPa, 之后充入 200 cm³/min 的 Ar 气, 并进行 30 min 的 Ar 离子清洗, 清洗完成后通入 20 min 的 20 cm³/min TMS 沉积粘结层, 最后通入 1 h 的 100 cm³/min 乙炔和 100 cm³/min Ar 气制备 DLC 膜层。

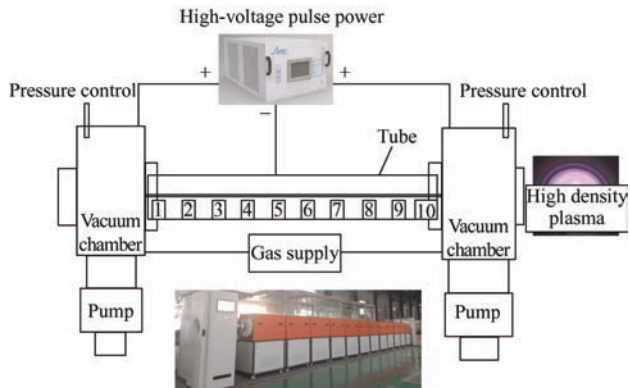


图 1 长管道内壁镀膜设备及原理示意图

Fig. 1 Schematic diagram and equipment of long tube deposition system for inner surface

1.2 膜层性能测试

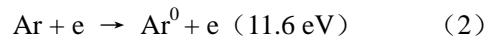
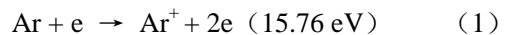
管道内壁膜层制备过程中, 采用光谱仪(AvaSpec-ULS2048CL-4-EV0)和光学聚焦平台对管道内 3 位置的 300~800 波段的等离子体光谱进行分析。膜层制备完成后, 采用色差仪进行膜层表面亮度测试, 确定膜层的 L*、a*、b*值, L*代表亮度, a*表示为红绿, b*表示为黄蓝。采用扫描电子显微镜(SEM, Gemini 300)观察膜层截面形貌。采用原子力显微镜(Bruker / Dimension Icon)测量膜层表面粗糙度。采用摩擦磨损试验机(MS-T3001)测试膜层耐磨性能, 选用直径 3 mm 的 GCr15 球为对磨副, 负载 3 N, 转速速度 200 r/min, 测试时间 120 min。采用纳米压痕硬度仪(Bruker TI980)进行膜层纳米硬度测试。采用水静态接触角测量仪(SDC-200SH)进行测量, 每次滴水 2 μl, 每片试样测试三次, 计算平均值为最终测试结果。采用激光

拉曼光谱仪(Horiba LabRam HREvolution)对膜层进行测量, 选用 532 nm 激光光源, 主要测量范围为 800~2 000 cm⁻¹, 并采用高斯曲线对拉曼光谱进行拟合分析。

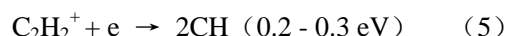
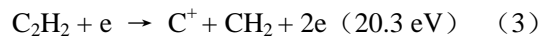
2 结果与讨论

2.1 管道内壁镀膜放电辉光光谱

在管内气体放电过程中, 管内放电区域中各粒子的光谱特性可以反映粒子的等离子体特征。基于等离子体光谱分析, 可得到工作气体离化的粒子种类、数量。在管道内壁镀膜工艺中, 第一步管内通入 Ar 气进行辉光放电清洗, 在 Ar 气放电过程中发生离化和激发^[15-16], 产生 Ar⁺和 Ar⁰, 如以下过程:



由式(1)、(2)可以得出, 电子能量较高时, 更有利于 Ar 的离化, Ar⁰(激发态波长大于 650 nm)、Ar⁺(电离态在 400~450 nm)^[17-18]数量增加较多, 而且 Ar⁺的增多有利于离化其他工作气体, 增强等离子体密度。工艺中乙炔被引入用来制备 DLC 膜层, 乙炔主要发生以下离化过程:



通过式(3)得出, 当电子能量较高时, 可以直接将乙炔离化成 C⁺; 而当电子能量较低时, 电子首先将乙炔离化成乙炔离子, 随后发生(4)和(5)过程, 生成 C₂、H 和 CH^[19], 如图 2 所示。

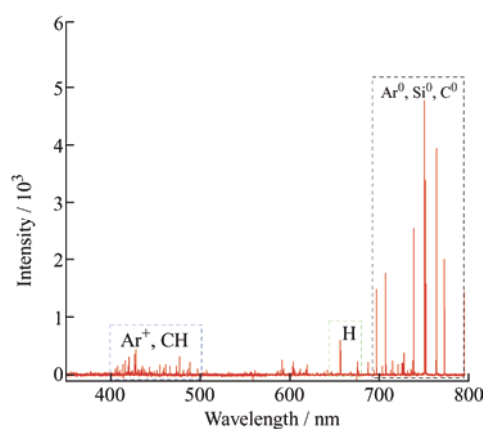


图 2 管道内 Ar+C₂H₂ 混合气氛的放电光谱

Fig. 2 Optical emission spectroscopy in the mixture of Ar+C₂H₂ in tube

2.2 管道内壁膜层截面形貌

通过 SEM 观察不同位置膜层的截面，如图 3 所示。膜层截面均匀致密，未出现裂纹、针孔等缺陷，膜层与基体结合过渡未出现裂纹。不同位置膜层厚度不同，1、3、7、9 位置的膜厚分别是 2.6、2.4、1.5、2.9 μm。靠近管道两端的膜层厚，说明该区域的等离子体密度高，且膜层的沉积速率高。

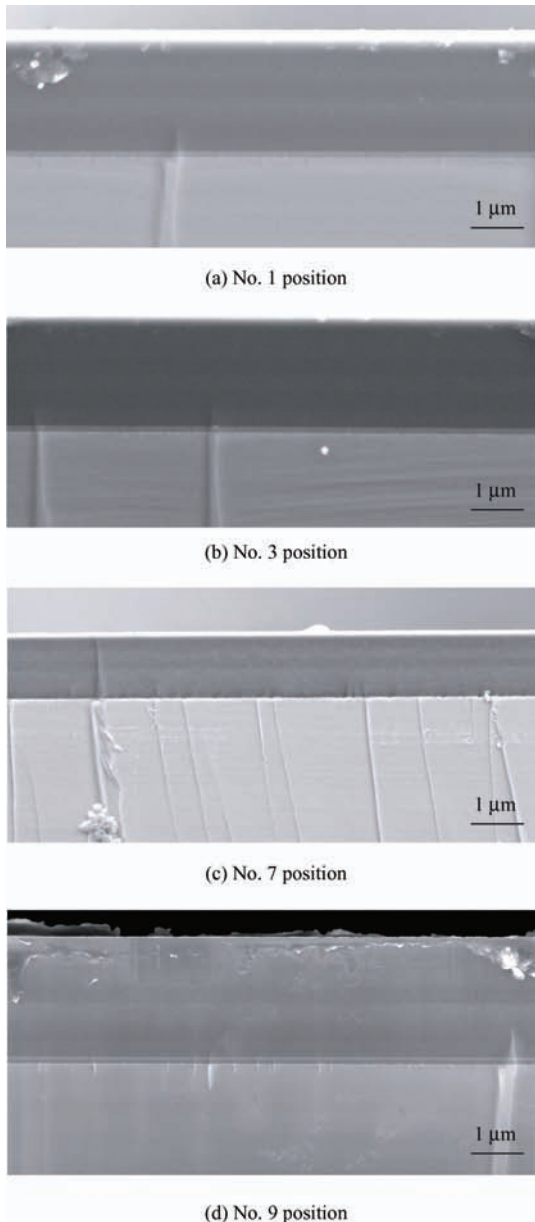


图 3 管内不同位置膜层横截面

Fig. 3 Cross sections of films at different positions inside the pipe

2.3 管道内壁膜层亮度

管道内壁膜层的均匀性直接影响着整个管道的膜层性能和管道的使用寿命，所以管道内壁膜层的均匀性十分重要。通过对试片膜层亮度的测试也可侧面反应出膜层性能的一致性。根据国际照明委员

会 (Commission Internationale De L'Eclairage, CIE) 确定的 L^* 、 a^* 、 b^* 颜色空间，两种颜色之间的总色差 ΔE^* 可以用式 (6) 计算^[20]：

$$\Delta E^* = [(\Delta L^*)^2 + (\Delta a^*)^2 + (\Delta b^*)^2]^{1/2} \quad (6)$$

如图 4 所示，采用分光光度计测量膜层的表面亮度 L^* 值。可以看出图中 9 位置的膜层的亮度值最大 37.4，管道两端亮度高于中间位置的亮度。3、7、9 位置与 1 位置的色差 ΔE^* 值分别为 1.8、1.9、1.84，说明膜层亮度均匀。

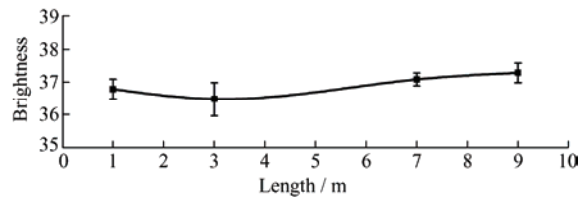
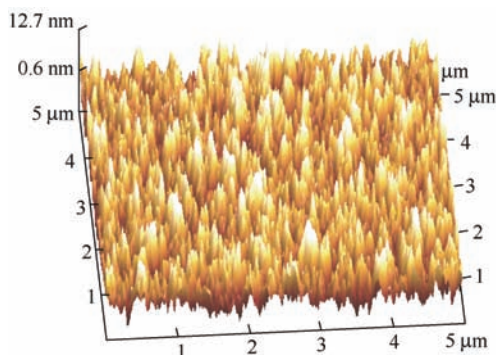


图 4 管内不同位置膜层表面 L^* 值

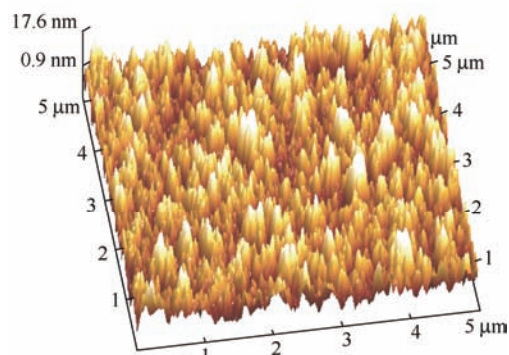
Fig. 4 Surface L^* values of films at different positions inside the tube

2.4 管道内壁膜层粗糙度

通过原子力显微镜测量膜层的表面粗糙度，以表示膜层表面的不平度。如图 5 所示，1、3、7、9 位置的膜层表面粗糙度分别是 2.82、3.91、3.25、2.58 nm。3 和 7 位置膜层表面有较多大的凸起，导致膜层表面粗糙度大；3 和 9 位置膜层表面凸起尺寸小，分布均匀。



(a) Surface topography of DLC films for No. 1 position



(b) Surface topography of DLC films for No. 3 position

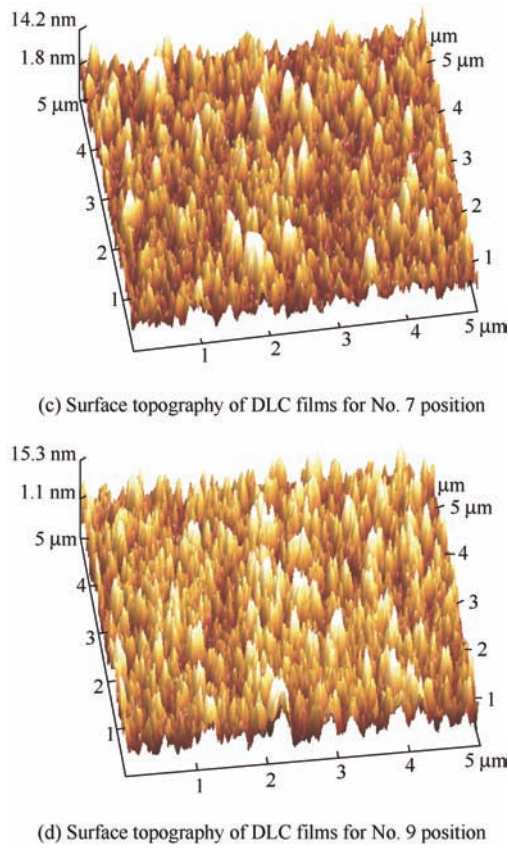


图 5 不同位置膜层表面形貌

Fig. 5 Surface morphology of films at different positions

2.5 管道内壁膜层水静态接触角

管道内部一般输送的是液态物质, 对管道内壁的水静态接触角有着特殊需求。如图 6 所示, 对管道内不同位置膜层表面的水静态接触角进行测量。水静态接触角的大小一般影响因素有膜层表面的微观结构、官能团和表面能等。结果显示, 在靠近管道两端(1、9 位置)膜层的水静态接触角小, 而靠近管道中间的膜层水静态接触角大。这可能是由于管道两端的等离子体密度高, 膜层表面受到的轰击强, 膜层表面较致密平滑^[21]。而中间位置的膜层表面受到轰击弱, 膜层表面的微观结构使得水静态接触角增大^[22]。

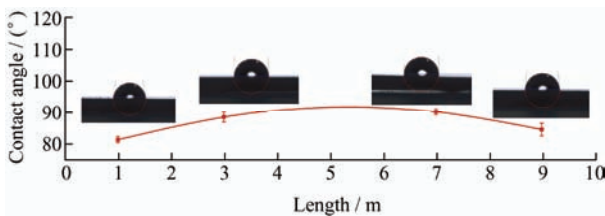


图 6 管内不同位置膜层表面接触角

Fig. 6 Contact angle of films at different positions inside the pipe

2.6 管道内壁镀膜磨损测试

管道内壁沉积镀膜的一个主要目的是提高管道内壁的耐磨性能。如图 7 所示, 对管道内 3 与 7 位置的试样膜层进行了 2 h 摩擦磨损测试。结果显示,

膜层的摩擦因数在开始的 20 min 内呈减小趋势, 从 0.225 降到 0.175 左右。随着时间延长, 摩擦因数基本稳定在 0.17, 这说明膜层在测试过程中, 膜层中石墨相在摩擦磨损过程中形成转移膜^[23], 为后续的磨损提供了润滑^[24-25]。对磨损后的磨痕进行观察, 未发现膜层破损剥落, 三维的磨痕形貌也可以看到磨痕中没有出现大的磨损坑, 如图 7、8 所示。通过式(7)计算比磨损率 I , 即单位滑动距离和单位负载产生的体积磨损量, 用于评估膜层的耐磨性。

$$I = \frac{A \cdot C}{S \cdot F_N} \quad (7)$$

式中, I 为比磨损率 (mm^3/Nm); A 为磨损轮廓的面积 (mm^2); C 为磨痕长度 (mm); S 为滑动距离 (m); F_N 为法向载荷 (N)^[26]。得到膜层的比磨损率 I 为 $8.9 \times 10^{-7} \text{ mm}^3/\text{Nm}$, 说明膜层的耐磨性较好^[27]。

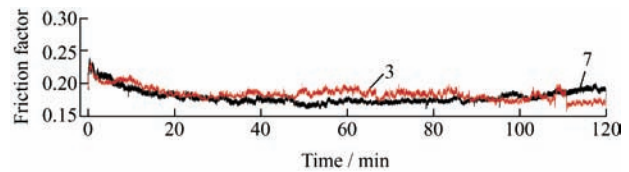
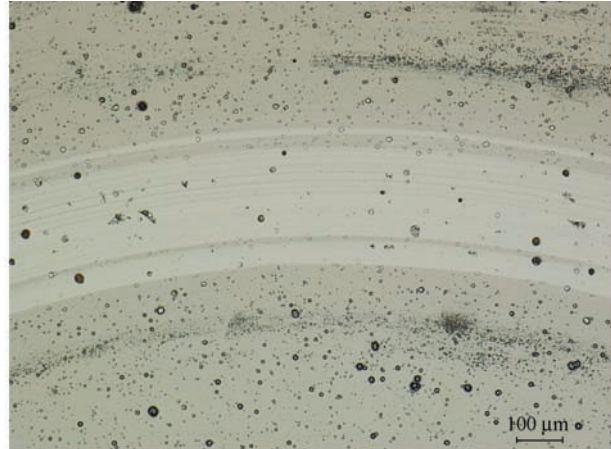
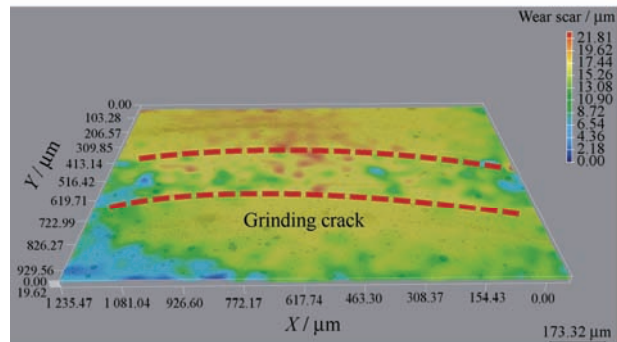


图 7 3 位置与 7 位置的膜层摩擦因数

Fig. 7 Friction factor of films at No. 3 and No. 7 positions



(a) Scratching of wearing for No. 3 position



(b) 3D morphology of wearing for No. 3 position

图 8 3 位置的试样磨痕及其三维形貌

Fig. 8 Scratching and 3D morphology of wearing for No. 3 position

2.7 管道内壁膜层硬度

图9是试样膜层的硬度与弹性模量曲线。发现膜层的硬度在管道两端较高,弹性模量也相对较高。这是因为在管道两端由于气体密度高,产生了高密度的等离子体,膜层得到强的离子轰击,使得膜层越致密,膜层的硬度也越高^[28]。在靠近管道中间位置的膜层硬度低。可能是由于管道中间位置的气体放电较弱,产生的等离子体密度低,造成沉积到薄膜表面的粒子能量低、轰击弱,从而导致制备的膜结构疏松、硬度低^[21]。

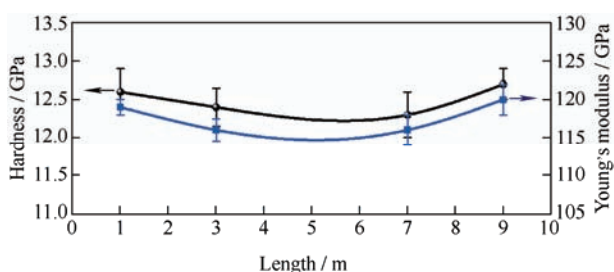
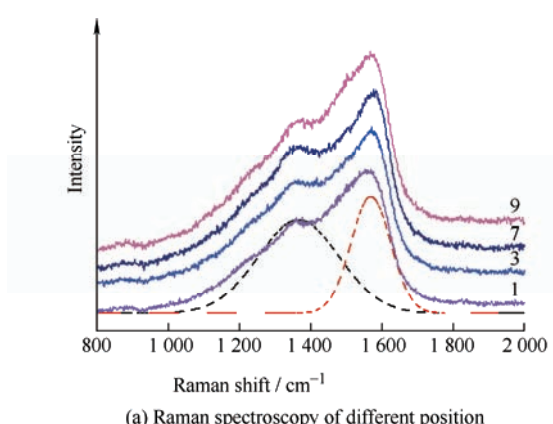


图9 不同位置膜层硬度与模量

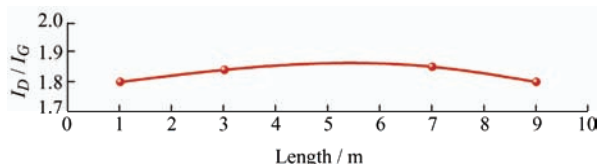
Fig. 9 Hardness and young's modulus of the film for different position

2.8 管道内壁膜层拉曼光谱分析

通过对膜层拉曼光谱进行分析,拉曼光谱被拟合成两个高斯波段,位于 1580 cm^{-1} 附近的主峰被指定为G峰,在 1350 cm^{-1} 附近的被指定为D峰^[29-31]。膜层的D峰和G峰的强度比值 I_D/I_G 可以用于表征DLC膜层中非晶态结构,G峰的位移表示膜层应力。图10 a所示不同位置膜层的拉曼光谱。与1和9位置对比,3和7位置G峰表现出向高峰位移动,说明两端的膜层应力高。图10 b所示膜层中 I_D/I_G 的分布趋势,管道两端的 I_D/I_G 低,说明两端的膜层中 sp^3 含量较高,且膜层硬度较高^[32-33]。



(a) Raman spectroscopy of different position



(b) I_D/I_G of different position

图10 管内膜层拉曼光谱

Fig. 10 Raman spectra of the inner film of the tubes

3 结论

采用实验室自主研制的管道内壁镀膜设备和电源,基于空心阴极放电产生的等离子体技术,在10 m管道内利用PECVD成功制备了DLC薄膜,解决了在大长径比管道内壁镀膜的难题,并研究了管道内气体放电辉光光谱及DLC膜层性能,主要结论包括:

(1) 实现在10 m大长管道内部的空心阴极等离子体放电,通过采集等离子体光谱,在管内发现的粒子包含 Ar^+ 、 C_2 、 CH 和激发态的 Ar^0 、 Si^0 、 C^0 。

(2) 管道内膜层的亮度和色差对比没有表现出较大差异。拉曼光谱结果表明,管道内膜层 I_D/I_G 均匀,说明在大长径比管道内壁沉积的膜层结构是均匀的,解决了在管道内部不均匀的问题。

(3) 获得DLC膜层硬度大于10 GPa。管道内膜层的磨损未出现破损脱落,表现出良好的耐磨性能,延长了管道的使用寿命。

参 考 文 献

- [1] 魏徐兵, 张明蓝, 王焱, 等. 304 不锈钢管内壁沉积耐磨防腐 DLC 涂层[J]. 表面技术, 2019, 48(9): 87-96.
WEI Xubing, ZHANG Minglan, WANG Yan, et al. Deposition of anti-corrosion and wear-resisting DLC coatings on inner wall of 304SS tube[J]. Surface Technology, 2019, 48(9): 87-96. (in Chinese)
- [2] WANNG T, YANG Y, SHAO T, et al. Simulation of magnetic-field-induced ion motion in vacuum arc deposition for inner surfaces of tubular workpiece[J]. Coatings, 2020, 10(11): 1053.
- [3] 韩峰. 约束电爆喷涂方法及机理研究[D]. 兰州: 兰州理工大学, 2019.
HAN Feng. Study on the process and mechanism of constrained electricalExplosion spraying[D]. Lanzhou: Lanzhou University of Technology, 2019. (in Chinese)

- [4] 杨浙. 小管径不锈钢管内壁多孔涂层喷涂控制[D]. 兰州: 兰州理工大学, 2022.
YANG Zhe. Study on the control and process analysis of the stainless steel pipe tube inner wall spraying with porous coating[D]. Lanzhou: Lanzhou University of Technology, 2022. (in Chinese)
- [5] 罗耀宗. 不锈钢管内表面镀铜[J]. 电镀与涂饰, 2005(7): 31-32.
LUO Yaozong. Copper plating on stainless steel pipe inner surface[J]. Electroplating and Finishing, 2005(7): 31-32. (in Chinese)
- [6] LUSK D, GORE M, BOARDMAN W, et al. Thick DLC films deposited by PECVD on the internal surface of cylindrical substrates[J]. Diamond and Related Materials, 2008, 17(7): 1613-1621.
- [7] PILLACA E, RAMIREZ M A, BEMAL J M G, et al. DLC deposition inside of a long tube by using the pulsed-DC PECVD process[J]. Surface and Coatings Technology, 2019, 359: 55-61.
- [8] 高凯晨, 刘仕远, 巩春志, 等. 细长管内表面镀 Cu 过程中的空心阴极辉光电[J]. 中国表面工程, 2022, 35(5): 264-271.
GAO Kaichen, LIU Shiyuan, GONG Chunzhi, et al. Glow discharge of hollow cathode during Cu plating on thin tube surface[J]. China Surface Engineering, 2022, 35(5): 264-271. (in Chinese)
- [9] WANG J, PU J, ZHANG G, et al. Interface architecture for superthick carbon-based films toward low internal stress and ultrahigh load-bearing capacity[J]. ACS Applied Materials & Interfaces, 2013, 5(11): 5015-5024.
- [10] BEWILOGUA K, HOFMANN D. History of diamond-like carbon films-from first experiments to worldwide applications[J]. Surface and Coatings Technology, 2014, 242: 214-225.
- [11] 李超, 马国佳, 孙刚, 等. 基体偏压对 316L 不锈钢表面多层 Ti-DLC 薄膜摩擦及腐蚀行为的影响[J]. 中国表面工程, 2023, 36(1): 189-199.
LI Chao, MA Guojia, SUN Gang, et al. Effects of substrate bias voltage on friction and corrosion behavior of multilayer Ti-DLC film on the surface of 316L stainless steel[J]. China Surface Engineering, 2023, 36(1): 189-199. (in Chinese)
- [12] PILLACA E, TRAVA-AIROLDI V J, RAMIREZ M A. Axial distribution improvements of DLC film on the inner surface of a long stainless steel tube[J]. Surface and Coatings Technology, 2021, 412: 126996.
- [13] WANG X, SUI X, ZHANG S, et al. Effect of deposition pressures on uniformity, mechanical and tribological properties of thick DLC coatings inside of a long pipe prepared by PECVD method[J]. Surface and Coatings Technology, 2019, 375: 150-157.
- [14] BABA K, HATABA R. Ion implantation into inner wall surface of a 1 m long steel tube by plasma source ion implantation[J]. Surface and Coatings Technology, 2000, 128: 112-115.
- [15] CAMERO M, GORDILLO-VAZQUEZ F J, GOMEZ-ALEIXANDRE C. Low-pressure PECVD of nanoparticles in carbon thin films from Ar / H₂ / C₂H₂ plasmas: synthesis of films and analysis of the electron energy distribution function[J]. Chemical Vapor Deposition, 2007, 13(6-7): 326-334.
- [16] GIELEN J W A M, VAN DE SANDEN M C M, SCHARM D C. Plasma beam deposited amorphous hydrogenated carbon: improved film quality at higher growth rate[J]. Applied Physics Letters, 1996, 152(69): 152-154.
- [17] MAIER, WILLIAM B. Dissociative ionization of molecules by rare-gas ion impact[J]. Journal of Chemical Physics, 1965, 42(5): 1790.
- [18] ASIM A, KOATAS S, MOHSIN R, et al. Principles for designing sputtering-based strategies for high-rate synthesis of dense and hard hydrogenated amorphous carbon thin films[J]. Diamond and Related Materials, 2014, 44(4): 117-122.
- [19] 胡健. 脉冲增强石墨阴极弧及其诱导辉光放电与碳基薄膜制备[D]. 哈尔滨: 哈尔滨工业大学, 2020.
HU Jian. Pulse enhanced graphite cathodic arc and its inducse glow discharge and preparation of carbon based films.[D]. Harbin: Harbin Institute of Technology. 2020. (in Chinese)
- [20] 马胜歌, 姜翠宁. 柱弧离子镀制备 Ti / TiN / Ti(N, C) / TiC 黑色硬质膜[J]. 真空科学与技术学报, 2006(4): 290-294.
- MA Shengge, JIANG Cuining. Growth of black hard films of Ti / TiN / Ti(N, C) / TiC cylindrical arc ion plating[J]. Journal of Vacuum Science and Technology, 2006(4): 290-294. (in Chinese)
- [21] 李超, 马国佳, 孙刚, 等. 基体偏压对 316L 不锈钢表面多层 Ti-DLC 薄膜摩擦及腐蚀行为的影响[J]. 中国表面工程, 2023, 36(1): 189-199.
LI Chao, MA Guojia, SUN Gang, et al. Effects of substrate bias voltage on friction and corrosion behavior

- of multilayer Ti-DLC film on the surface of 316L stainless steel[J]. China Surface Engineering, 2023, 36(1): 189-199. (in Chinese)
- [22] 于欣淼, 陈东旭, 霍婧雅, 等. 类金刚石膜对铝合金疏水结构耐久性能影响[J]. 真空科学与技术学报, 2022, 42(6): 475-481.
- YU Xinmiao, CHEN Dongxu, HUO Jingya, et al. Influence of diamond-like carbon film on the durability of hydrophobic structure of aluminum alloy[J]. Chinese Journal of Vacuum Science and Technology, 2022, 42(6): 475-481. (in Chinese)
- [23] KIM S J, YOON J I, MOON M W, et al. Frictional behavior on wrinkle patterns of diamond-like carbon films on soft polymer[J]. Diamond and Related Materials, 2012, 23: 61-65.
- [24] 王新宇, 张帅拓, 刘建, 等. 表面织构对管道内壁碳基涂层润湿性与摩擦学性能影响[J]. 摩擦学学报, 2021, 41(1): 86-94.
- WANG Xinyu, ZHANG Shuituo, LIU Jian, et al. Effect of surface texture on wettability and tribological properties of carbon-based coatings on the inner surface of pipes[J]. Tribology, 2021, 41(1): 86-94. (in Chinese)
- [25] WANG X, ZHOU H, ZHANG S, et al. The effect of acetylene flow rate on the uniform deposition of thick DLC coatings on the inner surface of pipes with different draw ratios[J]. Vacuum, 2022, 196: 110720.
- [26] 王海波, 赵君文, 陶星宇, 等. 高 Cu 铸造铝合金的摩擦磨损性能[J]. 材料工程, 2022, 50(11): 109-118.
- WANG Haibo, ZHAO Junwen, TAO Xingyu, et al. Friction and wear properties of cast aluminum alloy with high Cu content[J]. Journal of Materials Engineering, 2022, 50(11): 109-118. (in Chinese)
- [27] 曾群峰, 曹倩, ERDEMIR Ali, 等. 类金刚石膜超低摩擦行为的研究进展[J]. 中国表面工程, 2018, 31(4): 1-19.
- ZENG Qunfeng, CAO Qian, ERDEMIR Ali, et al. Current development situation of super low friction behavior of DLC films[J]. China Surface Engineering, 2018, 31(4): 1-19. (in Chinese)
- [28] 孙薇薇, 田修波, 李慕勤, 等. 偏压对自源笼形空心阴极放电制备 Si-DLC 薄膜结构和性能的影响[J]. 中国表面工程, 2019, 32(3): 69-79.
- SUN Weiwei, TIAN Xiubo, LI Muqin, et al. Effects of bias voltage on structure and property of Si-DLC films fabricated by self-source cage type hollow cathode discharge process[J]. China Surface Engineering, 2019, 32 (3): 69-79. (in Chinese)
- [29] 徐天杨, 詹华, 王亦奇, 等. 沉积气压与脉冲频率对内花键齿表面 Si-DLC 薄膜性能的影响[J]. 中国表面工程, 2022, 35(2): 243-252.
- XU Tianyang, ZHAN Hua, WANG Yiqi, et al. Effects of deposition pressure and pulse frequency on properties for Si-DLC films prepared on surface of internal spline tooth[J]. China Surface Engineering, 2022, 35(2): 243-252. (in Chinese)
- [30] WEI X, YIN P, WU J, et al. Deposition of DLC films on the inner wall of U-type pipes by hollow cathode PECVD[J]. Diamond and Related Materials, 2021, 114: 108308.
- [31] MABUCHI Y, HIGUCHI T, WEIHNACHT V. Effect of sp^2 / sp^3 bonding ratio and nitrogen content on friction properties of hydrogen-free DLC coatings[J]. Tribology international, 2013, 62: 130-140.
- [32] SANTOS N M, MARIANO S F M, UEDA M. Carbon films deposition as protective coating of titanium alloy tube using PIII&D system[J]. Surface and Coatings Technology, 2019, 375: 164-170.
- [33] IWAMOTO Y, HIRATA Y, TAKAMURA R, et al. Deposition phenomena of diamond-like carbon coating on inner surface of circular metal tube by nanopulse plasma chemical vapor deposition[J]. Diamond and Related Materials, 2022, 121: 108749.

作者简介: 靳朋礼, 男, 1990 年出生, 博士研究生。主要研究方向为等离子体镀膜。

E-mail: jinpengli332@163.com

田修波(通信作者), 男, 1969 年出生, 教授, 博士研究生导师。主要研究方向为等离子体镀膜。

E-mail: xiubotian@163.com